

"Reprinted (adapted) with permission from (*Energy Fuels*, 2012, 26 (11), pp 6584-6594  
DOI: 10.1021/ef301153b). Copyright © 2012 American Chemical Society  
Final Author's paper after peer review

## **The Effects of Different Dopants and Doping Procedures on the Reactivity of CaO-based Sorbents for CO<sub>2</sub> Capture**

Mohamad J. Al-Jeboori<sup>§</sup>, Paul S. Fennell<sup>§\*</sup>, Michaela Nguyen<sup>†</sup> and Ke Feng<sup>‡</sup>

<sup>§</sup> Department of Chemical Engineering and Chemical Technology, Imperial College London,  
London SW7 2AZ, UK.

<sup>†</sup> Department of Energy Process Engineering and Chemical Engineering,  
TU Bergakademie Freiberg, 09596 Freiberg, Germany.

<sup>‡</sup> King Abdullah University of Science and Technology, Thuwal 23955-6900, Kingdom of  
Saudi Arabia.

\*E-mail: p.fennell@imperial.ac.uk. Telephone: +44 (0) 20 7594 6637. Fax: +44 (0) 20 7594  
5638

**ABSTRACT:** Calcium-looping technology is a promising CO<sub>2</sub>-capture technology. The economics and environmental impact of the process are affected by the rapid decay in

reactivity of the limestone sorbent, which necessitates a high purge rate from the system to maintain sorbent reactivity. This work investigates techniques to improve long-term reactivity in such a system by doping the limestone with a variety of different dopants. It also demonstrates that the main reason for improvement is that the doping increases the volume of pores around 100 nm in diameter in the calcined material after a significant number of cycles, in comparison to the calcine from an undoped sorbent. Improved reactivity means a lower required purge-rate and potential disposal issues, and less fresh limestone to be used. Doped samples were subject to repeated cycles of carbonation and calcination in a Fluidised Bed Reactor (FBR). The work includes the use of inorganic salts  $MgCl_2$ ,  $CaCl_2$ ,  $Mg(NO_3)_2$  and the Grignard reagent-isopropylmagnesium chloride. Three types of doping procedures were explored; wet impregnation, solid mixing and quantitative wet impregnation. Experimental results showed that  $MgCl_2$ ,  $CaCl_2$  and Grignard reagents as dopants improved the carrying capacity of Havelock limestone.

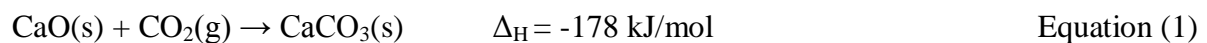
X-ray fluorescence (XRF) analysis of the doped samples after 13 cycles revealed that the number of dopant ions does not increase further with an increase in the doping concentrations above a critical value. Gas adsorption analyses showed that sorbents have a very small surface area-below  $4 \text{ m}^2/\text{g}$ , post-cycling. The pore size distribution appears to change significantly upon doping, and it is likely that optimising the pore size distribution upon cycling is one reason for the enhanced reactivity observed.

**Keywords:** “Calcium Looping”, “Doping”, “CO<sub>2</sub> capture”, “Fluidised Bed”, “Attrition”

## 1. INTRODUCTION

In the medium term, carbon dioxide capture and storage (CCS) is an essential technology to reduce the emission of CO<sub>2</sub> through its capture from fossil fuel-fired power plants. It is

necessary to produce a concentrated stream of CO<sub>2</sub><sup>1-3</sup> prior to compression. Several technologies have been suggested to capture the CO<sub>2</sub> from the exhaust stream and produce a concentrated stream suitable for compression and finally sequestration, including the "Calcium Looping Cycle" (Ca-looping).<sup>4,5</sup> This technology is currently under investigation at the 1.7 MWth-scale as part of the EU CaOling project, with the pilot-scale circulating fluidised bed at the heart of the project demonstrating continuous > 90 % CO<sub>2</sub> capture for periods of up to 12 hours within the first 3 months of operation.<sup>6</sup> In this technique, a calcium-based sorbent is repeatedly circulated between two reactors – the carbonator and the calciner. The main chemical reaction, on which this process is based, is the reversible reaction of calcium oxide with carbon dioxide, presented in equation 1:



Carbonation of CaO (equation 1) takes the CO<sub>2</sub> out of the gas stream at around 650 – 700 °C. After passing the formed CaCO<sub>3</sub> to the calciner, the reverse reaction occurs at a higher temperature (850 – 950°C) and a highly concentrated carbon dioxide stream is released. The main drawback while using this method of CO<sub>2</sub> capture is the loss of reactivity of sorbent upon cycling. The decrease in the reactivity of sorbent is affected by: sorbent sintering that causes an increase of density of particles and pore closure/ loss and reduction of the reacting surface area;<sup>7</sup> loss of material through attrition; and competing reactions of the sorbent with sulphurous compounds and ash fouling.<sup>8</sup> Several research groups have studied and explored different ways to improve long-term sorbent reactivity in the calcium looping cycle. Methods explored include improving the reactive porosity and/or improving the mechanical stability of sorbents. These investigations include: thermal preactivation of fresh sorbent;<sup>9,10</sup> hydration or

steam of unreactive sorbent;<sup>11,12</sup> sorbent modification using acetic acid;<sup>13</sup> synthesis of novel CaO-based sorbents;<sup>14</sup> and doping of natural sorbents.<sup>15</sup>

Doping of natural sorbents can improve the reactivity of these materials by reducing the rate of decay of reactivity and/or enhancing the residual reactivity. The advantage of doping is that it can be a relatively cheap method of improving a sorbent – a key advantage of the Ca-looping process is that it uses a very cheap starting material (essentially, crushed rock), so that any activation strategy should not be overly costly.

Different dopants and doping methods have previously been tested to overcome the degradation of the natural sorbents with cycling. The impregnation of limestone with aqueous solutions (0.002 – 0.100 M) of different salts such as Na<sub>2</sub>CO<sub>3</sub> or NaCl was found to show a small improvement in long-term reactivity,<sup>15</sup> even though doping limestone with high concentrations of the aqueous solution of Na<sub>2</sub>CO<sub>3</sub> or NaCl showed a decrease in overall reactivity.<sup>16</sup> Several alkali metal dopants were used by Reddy *et al*<sup>17</sup> to investigate the behaviour of CaO upon calcium looping. They found that cesium-doped calcium oxide sorbents showed the best improvement in the carrying capacity. Recently, a large number of additives and dopants were tested for their effect on the carrying capacity of sorbents. Li *et al*<sup>18</sup> determined an optimal addition amount of 0.5 – 0.8 wt-% KMnO<sub>4</sub> to provide an ideal carbonation conversion during long term calcination/carbonation cycles. They observed that particles of calcined KMnO<sub>4</sub>-doped limestone are more stable than particles of the untreated sorbent. Elzinga *et al*<sup>19</sup> investigated the role of Mg-based precursors for the enhancement of the carrying capacity of several thermally preactivated CaO sorbents while using wet impregnation. They reported that Mg(NO<sub>3</sub>)<sub>2</sub>-doped calcium oxide sorbent is the most promising with an increase in initial stability and improved cyclic stability.

The utility of doping to raise the long-term reactivity of Ca-based sorbents has thus already been demonstrated. Here, we have studied the role of a range of different dopants and doping

methods (wet impregnation, solid mixing salt and quantitative wet impregnation) on the enhancement of the reactivity of different limestones: Havelock (Canada) and Purbeck (U.K.), including the calcined form of these limestones. Initially, our focus was doping with different Mg-salts, since we believed that these would partially dolomitise the limestone, leading to improved reactivity. However, the experiments led to a greater focus on the effects of the doping anion on the reactivity. Our study includes the use of inorganic salts  $\text{MgCl}_2$ ,  $\text{CaCl}_2$ ,  $\text{Mg}(\text{NO}_3)_2$  and Grignard reagent-isopropylmagnesium chloride. Furthermore, magnesium chloride doping was carried out by a wet impregnation method using  $\text{MgCl}_2$  solutions of concentrations between 0.05-0.50 M solutions, a simple mixing of the particles and a solid salt, and a quantitative wet impregnation method. In addition, the effect of high pressure (up to 10 bar) of wet impregnation doping on the improvement of sorbent performance was studied using  $\text{MgCl}_2$  solutions of concentrations between 0.02-0.05 M solutions. This work aimed to determine if the positive effect of doping could be associated to either the cation or the anion of the salt used, and also to investigate the mechanism by which positive effects are produced. The investigation includes the use of  $\text{MgCl}_2$ , Grignard reagent and  $\text{Mg}(\text{NO}_3)_2$  to examine the effect of the  $\text{Cl}^-$  anion on the enhancement of the carrying capacity. The use of  $\text{CaCl}_2$  dopant was to provide  $\text{Cl}^-$  in a form other than  $\text{MgCl}_2$  or Grignard reagent; this was to verify that the enhancement in carrying capacity was due to presence of the  $\text{Cl}^-$  anion rather than the  $\text{Mg}^{2+}$  cation. The Grignard reagent in tetrahydrofuran (THF) was used to allow doping of  $\text{CaO}$  (i.e. to provide an anhydrous route to doping, preventing the formation of  $\text{Ca}(\text{OH})_2$  from the calcined material when doped). The doped samples were subjected to repeated cycles of carbonation and calcination in a Fluidised Bed Reactor (FBR), and the results obtained were compared with the corresponding undoped limestone. One significant advantage of using a fluidised bed reactor was that the sample of limestone used in the FBR was significantly larger than that used in a TGA experiment allowing the recovery

of sufficient particles of limestone after each experiment to enable various analytical techniques to be used.<sup>15</sup>

## **2. EXPERIMENTAL SECTION**

**2.1. Materials.** Inorganic salts and isopropylmagnesium chloride 2M in tetrahydrofuran (THF) were purchased from Fisher Scientific and Acros Organics. Prior to the doping procedure,  $\text{MgCl}_2 \cdot 6\text{H}_2\text{O}$  and  $\text{Mg}(\text{NO}_3)_2 \cdot 6\text{H}_2\text{O}$  were dried in an oven at 373 K for 8 h. The number of remaining water molecules of hydration was confirmed by TGA to be 4 ( $\text{MgCl}_2 \cdot 4\text{H}_2\text{O}$ ,  $\text{Mg}(\text{NO}_3)_2 \cdot 4\text{H}_2\text{O}$ ).  $\text{CaCl}_2$  was purchased as anhydrous salt and due to its hygroscopic behaviour water molecules from the atmosphere remained associated with the salt upon drying after doping.

**2.2. Physical measurements.** A Perkin-Elmer FTIR-Spectrum100 spectrophotometer equipped with a 10 cm length gas cell with NaCl plates was used to detect  $\text{CO}_2$  in the off gas of the reactor. Semi-quantitative XRF analysis for samples was recorded using a Bruker XRF Explorer-S4 analyser. Brunauer-Emmett-Teller (BET) surface areas and pore volume distributions were determined using a Micromeritics Tristar 3000  $\text{N}_2$  sorption analyser. SEM (Scanning electron microscope) analysis was conducted using (SEM; JEOL 5800).

**2.3. Description of the experimental set-up.** Experiments were performed in a laboratory scale atmospheric pressure Fluidised Bed Reactor (FBR), as shown in Figure 1. The reactor consists of a quartz reaction vessel heated by an external resistance heated tube furnace, based on systems described elsewhere.<sup>20</sup>

**Figure 1 can be placed after paragraph.**

The furnace tube is made of Incoloy (I.D. 26.25 mm, O.D. 33.4 mm, length 430 mm). The furnace is supplied by a transformer (1600 A, 2 V) through two sets of 10 copper cables (35 mm<sup>2</sup> cross-section, 800 mm length) to two moveable copper electrodes, separated by 180 mm, bolted to the tube. The copper cables connecting the electrodes and the transformer are cooled by water passing through 1/8" copper tubing coiled around them, and all exposed parts of the quartz vessel, together with the electrodes and furnace tube are insulated using Superwool 607 Max Blanket.

The reactor comprises a quartz reaction vessel (25.50 mm, O.D., length 543 mm) with a small sintered quartz plate 200 mm from the base supporting a fluidised bed of sand. The temperature of both the bed and the outer reactor wall are measured using type 'K' thermocouples and controlled using a modified PID controller, using a computer program written in Agilent VEE Pro 7.0 software.

**2.4. Doping of Particles.** Three types of doping techniques were explored in this study (see Supporting Information, ESI, for the solid mixing procedure and results for carbonated limestone):

*2.4.1. Wet Impregnation.* The doping method used prior to cycling experiments as described in previous work<sup>15</sup> was as follows: An aqueous solution of the salt (of a known molarity) and 16 g of limestone (500-710  $\mu\text{m}$ ) were added to a flask containing 600 mL of the solution. The flask was gently swirled to mix the contents before sealing. It was then left for 40 h before the contents were gently shaken (to suspend fines) and the liquid was decanted off including any fines (which were a very small proportion of the total solids). The remaining solids were washed onto a watch glass using the same solution. The solids were

then dried in an oven at 373 K for 12 hours, before being transferred and sealed in a container. A control experiment was conducted in which Havelock limestone particles were simply washed with distilled water according to the procedure outlined above. It showed no deviation from a standard experiment without washing.

*2.4.2. Quantitative Wet Impregnation.* To combine the simplicity of solid mixing and the homogenous distribution and accuracy of wet impregnation, a quantitative wet impregnation method was developed. In this method, limestone and salt were weighed as described for solid mixing, but before mixing them, the salt was dissolved in 2 mL DI water, thoroughly shaken and poured over the limestone. A similar procedure was implemented when Grignard reagent was used as a dopant, but with 2 mL THF instead of DI water (this could be used for both CaO and CaCO<sub>3</sub>). For both methods, the petri dish with the doped sample was dried in an oven at 373 K for one hour and then stored in a desiccator.

*2.4.3. Calculation of Residual Carrying Capacity: The Grasa Equation.* Grasa *et al*<sup>21</sup> proposed a semi empirical equation to model the decay of the carrying capacity of a sorbent. This is similar to that originally used in modelling other sintering processes.

$$X_N = \frac{1}{\frac{1}{1 - X_r} + kN} + X_r \quad \text{Equation (2)}$$

In this equation,  $X_N$  describes the carrying capacity after N cycles,  $X_r$  the residual reactivity and k the deactivation constant. The residual reactivity describes the carrying capacity of the sorbent after a large number of cycles, which Grasa suggested to be around 500 cycles. That number is justified by experimental data, which showed that the carrying capacity loss evened out after about 50 cycles. The carbonation conversion was almost constant between 50 and 500 cycles and was set to be the residual conversion. The deactivation constant k



describes the rate of decay, i.e. how fast the carrying capacity reduces to the residual carrying capacity.

## 2.5. Experimental Procedure

2.5.1. *Standard Cycling Conditions.* Standard experiments were carried out with an inlet gas concentration of  $\approx 15\%$  v/v CO<sub>2</sub>, balance N<sub>2</sub>, a CO<sub>2</sub> concentration typical of flue gases, at atmospheric pressure. The calcination was in general conducted at 1173 K and carbonation at 973 K. All glass/quartzware was washed thoroughly in preparation for each experiment. Each experiment utilised 8 mL of quartz sand, levelled and weighed ( $\sim 12.00$  g), of size fraction 355-425  $\mu\text{m}$ . The sand was to support and to ensure a direct and homogenous heat transfer to every limestone particle, but also to act as a thermal bath, preventing significant heating or cooling of the bed caused by the reaction enthalpy of carbonation or calcination. The cold flow rate of gas entering the reactor was set by calibrated rotameters to 47.5 cm<sup>3</sup>/s at 1 bar<sub>a</sub>, which corresponds to  $U/U_{\text{mf}} = 11.5$  (estimated using the correlation of Wen and Yu<sup>22</sup>) for sand of size fraction 355-425  $\mu\text{m}$  in a N<sub>2</sub> atmosphere at 1173 K, to ensure vigorous fluidisation. The reactor (with the sand added) was heated to the calcination temperature under a N<sub>2</sub> atmosphere. Prior to each experiment, calibration gas (containing 15 vol % CO<sub>2</sub> in N<sub>2</sub>, Air Liquide) was passed through the bed to calibrate the FTIR gas analyzer. When at temperature, the gas was switched to the reaction gas (15.00 % v/v CO<sub>2</sub>, balance N<sub>2</sub>, BOC) and the concentration of CO<sub>2</sub> in the off-gas was measured continuously by an FTIR gas analyser *via* a sampling system containing glass wool and calcium chloride to filter out fine particles and humidity. Once a stable CO<sub>2</sub> concentration was achieved,  $4.05 \pm 0.02$  g of limestone of size fraction 500-710  $\mu\text{m}$  (to allow easy separation by sieving of the limestone from the sand) was added to the reactor. After addition of the limestone, the bed was held at the calcination temperature for 600 s before being cycled between the carbonation and calcination temperatures with the setpoint being held at 600 s for each, allowing full

calcination on each cycle and carbonation to proceed past the reaction-limited regime. Experiments were performed for 13 and 50 (for promising dopants) cycles of calcination and carbonation. After the 14th or 51st calcination, the gas supply was switched to pure N<sub>2</sub>, the sample was cooled to around 400°C and removed and placed in a crucible within a desiccator, and weighed while hot to prevent hydration. The sample was then placed into an air-tight jar, sealed with Parafilm and stored in a desiccator for further analysis. Contact with ambient air was avoided as much as possible to prevent hydration of the sample. The number of experiments was varied between 1 and 3 for each point, with 3 experiments conducted for the most promising doping concentrations.

## **2.6. Characteristics of Initial Materials.**

*2.6.1. XRF Analysis.* The composition of each limestone was determined by XRF analysis for Havelock and Purbeck. The original composition of the utilized limestones is summarised and compared in Table 1.

**Table 1 can be placed after this paragraph**

*2.6.2. SEM Analysis.* The distribution of Mg and Cl elements in one doped limestone was measured. The MgCl<sub>2</sub>-doped Havelock limestone particles were embedded in epoxy resin, cross-sectioned, ground and polished. Then the section was scanned by SEM.

*2.6.3. Gas Adsorption Analysis.* Measurements were conducted with a TriStar 3000 – surface area and porosity analyser, which resulted in the determination of the surface area by the Brunauer-Emmett-Teller (BET) equation<sup>23</sup> and the pore size and volume distribution by Barrett-Joyner-Halenda (BJH) analysis.<sup>24</sup> For this analysis, about 0.17 g of the limestone particles, sieved from the limestone-sand mixture, were used.

## **3. RESULTS**

From Table 1, some aspects are notable in direct comparison of the initial limestones. First of all, the limestones have differences in purity. Purbeck has more silica impurities (much of this silica is present as small flint particles). Furthermore, Purbeck has a higher magnesium, iron and aluminium content and contains sulphur and phosphorous.

**3.1. Doping Methods.** The effects of the individual procedures (wet impregnation and quantitative wet impregnation) on Havelock limestone, doped with magnesium chloride are presented in Figure 2, for the best results obtained. The equation of Grasa *et al*<sup>21</sup> (equation 2) is also plotted in Figure 2. The most important results for carrying capacity, etc, for this work are shown in Table 2. However, the results of all experiments conducted (a significantly enhanced data set) are presented in Table SI 2.

**Figure 2 can be placed after this paragraph.**

The impact of different concentrations of  $\text{MgCl}_2$  doping solutions, utilising wet impregnation, has previously been described.<sup>3,25</sup> The best result gave a concentration of 0.05 M with a residual reactivity ( $X_r$ ) of 0.15, which is immense considerable improvement compared to ~ 0.03 for the undoped Havelock limestone. A quantitative wet impregnation doping technique with the same mass of  $\text{MgCl}_2$  dopant was explored, which showed a residual reactivity of 0.14, Table 2 shows the effect of doping methods and type of dopant on the experimental parameters investigated. As a result, this doping method was preferred for all other doping experiments because it is a good compromise between the simplicity of dry mixing and the time required for wet impregnation. A limited number of experiments were conducted where doping was conducted at pressures of up to 10 bar. These showed similar results to those for quantitative wet impregnation (Figure SI 1). Indeed, simply mixing the dry powders led to some increase in reactivity (see Supporting Information, Table SI 1).

**3.2. Havelock Limestone Doped with Different Salts.** The Havelock limestone was modified with 4 different dopants at different concentrations, Table 2. Unmodified Havelock is the limestone with the highest propensity for mass loss of the considered limestones, about 20 % over 13 cycles, and its reactivity dropped rapidly to a carrying capacity of 10 % after 13 calcination/carbonation cycles.

**3.3. Variation of Dopant.** The long-term performance of Havelock limestone was significantly improved by adding small concentrations of different dopants using quantitative wet impregnation, the best result for each dopant is shown in Figure 3.

**Figure 3 can be placed after this paragraph.**

It can be seen that every dopant improves the performance of the limestone to a certain degree, but there are considerable differences in the extent and properties of this enhancement. Obviously,  $\text{MgCl}_2$ ,  $\text{CaCl}_2$  and the Grignard reagent raise the residual reactivity of Havelock (as derived from the equation of Grasa) from  $\sim 0.03$  to 0.14, 0.13 and 0.13, respectively. The enhancement of  $\text{Mg}(\text{NO}_3)_2$  is minor as the residual reactivity is only improved by  $\sim 2\%$  (from 0.03 to 0.054).

**3.4. Variation of Doping Concentration.** For each dopant a different doping concentration showed the best results. If almost the same doping concentration of ca. 0.165 mole-% for every dopant is viewed, the trends of Figure 3 are inconclusive. As the amount of dopant was found to have a significant effect on the cycling behaviour of the sorbent for each dopant,<sup>12,15,18</sup> a range of concentrations was tested to determine the optimal addition, (Figure 4 and Table 2). However, it has to be pointed out that the “best” result was defined by the highest residual reactivity ( $X_r$ ) and does not always correspond to the apparent trend of the

plot. Error bars, corresponding to one standard deviation, are shown in Figure 4. It is clear that the reproducibility is high for these experiments, but that experiments with very high dopant concentrations have the worst reproducibility (owing to the potential for agglomeration of the bed).

**Figure 4 can be placed after this paragraph.**

In general, it is clear that for every dopant an optimal doping concentration exists where the improvement in reactivity is most significant. In the experiments for Havelock limestone, this doping concentration is in most cases around 0.14 - 0.165 mole-%. For all concentrations above or below this point, the long-term reactivity is lower. Doping of Havelock limestone with a relatively high concentration of 0.755 mole-% magnesium chloride even reduced the initial reactivity of the sorbent, (Figure 4). Although the Grasa plot does not follow the produced data very well (due to the aforementioned problem with plotting for the highest or lowest sorbent degradation), an intense drop in CO<sub>2</sub> capture ability is seen. Lower concentrations, on the contrary, improve the carrying capacity. The same effect was earlier seen by Fennell *et al* for limestone doping with Na<sub>2</sub>CO<sub>3</sub> and NaCl and Gonzalez *et al* for KCl and K<sub>2</sub>CO<sub>3</sub>.<sup>15,25</sup> In attempts to understand the mechanisms of doping, both phenomena, the increase of reactivity through doping and the potential for higher deterioration at larger concentrations, need to be understood concurrently.

**Table 2 can be placed after this paragraph.**

**3.5. Behaviour of Havelock After 50 Cycles.** The behaviour of an undoped Havelock limestone and the doped Havelock with 0.165 mole-% MgCl<sub>2</sub> over 50 cycles were studied. The doped Havelock with MgCl<sub>2</sub> raises the residual reactivity of Havelock (as derived from the equation of Grasa) from 0.04 to ~ 0.11, Figure 5.

**Figure 5 can be placed after this paragraph.**

**3.6. Purbeck Doped with Different Salts.** Purbeck limestone was subjected to the same dopants as Havelock limestone and again for every type of dopant a range of different concentrations was tested. Purbeck limestone was doped with  $\text{MgCl}_2$ ,  $\text{CaCl}_2$  and  $\text{Mg}(\text{NO}_3)_2$ . The aim was to see if there is any effect on sorbent performance when doping with a concentration which showed most promising results on Havelock. There was no improvement realised with the  $\text{MgCl}_2$  and  $\text{CaCl}_2$  dopants (Figure 6). The enhancement was not as impressive as for Havelock, which could be simply due to the fact that Purbeck has a considerably higher initial long-term reactivity, potentially because of its more favourable initial pore size distribution (which discussed later).

**Figure 6 can be placed after this paragraph.**

The focus was slightly shifted from intense investigation of chloride salts doping on Havelock towards a stronger focus on nitrate doped Purbeck. Magnesium nitrate appeared to have a more significant effect on Purbeck than on Havelock. The sequence of improvement of dopants for Purbeck was as follows:  $\text{Mg}(\text{NO}_3)_2 > \text{MgCl}_2 = \text{CaCl}_2$ . The optimal doping with magnesium nitrate showed residual reactivity of 0.16 and it therefore had a marginal effect, compared to a value of 0.14 for unmodified Purbeck sorbent.

**3.7. XRF Analysis.** XRF analysis was conducted (see Table 2) to investigate the fate of the material doped into the particles. For Havelock limestone there was an emphasis on dopants with the chloride anion (to determine the retention of the anion in the crystalline matrix), while for Purbeck, the focus was on doping with magnesium nitrate.

**3.8. Carbonated and Precalcined Havelock Doped with  $\text{MgCl}_2$ ,  $\text{CaCl}_2$  and Grignard Reagent.** Different dopants for Havelock limestone:  $\text{MgCl}_2$ ,  $\text{CaCl}_2$  and Grignard reagent to

doped the precalcined form of limestone - CaO were investigated. Two different doping techniques were used, solid mixing (see Supporting Information) with MgCl<sub>2</sub>, CaCl<sub>2</sub> and quantitative wet impregnation doping with Grignard reagent were performed on the carbonated form-CaCO<sub>3</sub> and the precalcined form-CaO. Upon cycling, doped Havelock in the carbonated form-CaCO<sub>3</sub> and precalcined form-CaO showed an improvement in the carrying capacity of CO<sub>2</sub> in comparison with the undoped Havelock, Figure 7. However, doped precalcined Havelock showed higher mass loss in comparison with the undoped limestone after 13 cycles, Table 2.

Solid mixing doping of the carbonated form of Havelock with MgCl<sub>2</sub> and CaCl<sub>2</sub> exhibited an optimal ratio of 0.165 and 0.138 mole-%, respectively (mole ratio of dopant to sorbent %). A remaining residual reactivity of 0.13 and 0.12 for MgCl<sub>2</sub> and CaCl<sub>2</sub>, respectively, (Equation 2) was observed after a large number of cycles (Table SI 1).

**Figure 7 can be placed after this paragraph.**

XRF analysis (Table 3) for cycled samples of carbonated doped Havelock with 0.165, 0.138 and 0.150 mole-% of MgCl<sub>2</sub>, CaCl<sub>2</sub>, and Grignard reagent, respectively, showed the presence of Cl<sup>-</sup> anion after 13 cycles. XRF data revealed that the composition of the sorbent stays basically unaltered with cycling, except there is an amount of about 0.060-0.067 mole-% of Cl<sup>-</sup> anion doped into the sample and a reduction of the amount of potassium remaining in the sample to 0.017-0.023 mole-% after 13 cycles.

**Table 3 can be placed after this paragraph.**

Interestingly, XRF analysis for cycled doped precalcined samples showed no Cl<sup>-</sup> anion retained in the limestone after 13 cycles (see Table 2).

For doped Havelock in the carbonated form, the curve after 13 cycles shows that after reaching the most improving doping concentration (0.165, 0.138 mole-% for MgCl<sub>2</sub>, CaCl<sub>2</sub>,

respectively and 0.15 mole-% for Grignard reagent), the amount of  $\text{Cl}^-$  ions does not increase further with increasing doping concentration (see Supporting Information, Figure SI 2).

**3.9. Purbeck Doped with  $\text{Mg}(\text{NO}_3)_2$ .** The results for Purbeck doped with the best doping concentrations of 0.19 mole-%  $\text{Mg}(\text{NO}_3)_2$  as well as the variation of doping concentration for  $\text{Mg}(\text{NO}_3)_2$  is shown in Figure 8.

**Figure 8 can be placed after this paragraph.**

There are few changes in the composition of Purbeck limestone with cycling, Table 4. As expected, the content of magnesium increases with doping concentration of magnesium nitrate and is interestingly highest at the point where the improvement of cycling performance is most significant, though the increase is small. However, undoped Purbeck limestone exhibits a high asymptotic activity compared with that of the Havelock. The residual reactivity of undoped Purbeck limestone was 0.14 while undoped Havelock limestone showed a residual reactivity of  $\sim 0.03$ . This means that this doping technique may be most useful if a limestone local to a power plant is found to have low reactivity; some limestones may not significantly benefit from the technique.

**Table 4 can be placed here.**

**3.10. Gas Adsorption Analysis.** BJH pore volumes (for pores in the size range 3-150 nm) were determined for each calcined limestone after 13 cycles. Results are shown in Figure 9, which indicates the doping concentrations resulting in the highest or the lowest residual reactivity after reaction.



**Figure 9 can be placed after this paragraph.**

Typical results of the distribution of volume inside pores of different widths are shown in Figure 10. Examination of Figure 9A reveals that, after doping with 0.165 mole %  $\text{MgCl}_2$ , a large volume in pores less than 20 nm closes up. The pore diameters more than 30 nm appear to shift upward to higher pore diameters. It is clear that the greater the extent of doping, the greater the shift of the porosity to larger diameters. The most interesting feature of Figure 9A is that, there remains a substantial volume of pores with diameters between 100 and 150 nm.

The measured surface area for the undoped calcined Havelock was  $2.4 \text{ m}^2/\text{g}$  (Figure 10). The BET surface area for Havelock doped limestone with  $\text{MgCl}_2$  was derived for each concentration, showing an increase in surface area with 0.165-%  $\text{MgCl}_2$  doped and a drop after reaching 0.76-%  $\text{MgCl}_2$ . However, Purbeck limestone doped with  $\text{Mg}(\text{NO}_3)_2$  (see Figure 9B) in the range 0.1–0.19 mole-% showed a similar trend in which the pore diameters greater than 30 nm appears to shift upward. In addition, an increase in the BET surface area was observed compared with the undoped limestone.

**Figure 10 can be placed after this paragraph.**

**3.11. SEM Analysis.** SEM analysis was performed to determine the distribution pattern of dopant material within doped limestone particles, Figure 11. The elements Mg and Cl appeared at all scanning points simultaneously. Because the distribution of elements can represent the distribution of  $\text{MgCl}_2$  in doped limestone, this shows that a small amount of Cl penetrates into the middle of the particles. The results show that elemental concentrations can vary greatly below the surface of the particles (i.e. that the doping may not proceed uniformly throughout the particles). These results led us to the (erroneous) conclusion that the doping

of calcined materials, owing to the greater porosity (and hence greater potential for dopants to reach the centre of the particle), was likely to improve the overall reactivity. This was the reason for studying the doping of calcined materials utilising the Grignard reagent.

**Figure 11 can be placed after this paragraph.**

**3.12. Attrition.** Attrition is, besides sintering, one of two main mechanisms that cause a loss in reactivity. However, unless a limestone is particularly prone to attrition, by far the greatest cause of loss of reactivity is from sintering. Attrition is a particle size reduction by grinding of fine material from the surface of a particle, with (here) fines immediately entrained from the fluidised bed. As was proposed earlier, the positive effect of doping on the friability of the sorbent is likely to be revealed in a diminishing mass loss with increasing doping concentration. This has been seen already in previous work.<sup>25</sup> For Havelock limestone, the mass loss monotonically decreases with increasing doping concentration. A clear tendency can be seen for dopants that the mass loss decreases as soon as the dopant is introduced and is further reduced if a higher amount of dopant is added. For Purbeck however, this trend is not exhibited. In general, a slight increase in mass loss was observed. This could be due to the fact, that the mass loss for this limestone is initially much lower than for undoped Havelock, which loses more than 20 % of its mass after 260 min of cycling (Figure 12). On the other hand, Purbeck only loses 3 % of its mass over the same time period. In comparison, a limestone would lose more than 80 % of its reactivity from sintering over the same period.

**Figure 12 can be placed after this paragraph.**

## 4. DISCUSSION

The aim of this experimental work was to explore and to develop inexpensive and simple doping methods and dopant materials to improve the CO<sub>2</sub> carrying capacity of the sorbent, and also to elucidate the mechanism by which such doping works. However, the effect of steam and SO<sub>2</sub> on the performance of doped samples has not been included; they are clearly important topics for further work.

Experimental data has shown that doping has a positive impact on both reactivity and attrition. It was found that a high doping concentration significantly reduced attrition but caused a drop in the reactivity. The low doping concentration also had a positive impact on attrition and significantly improved the reactivity. However, at lower concentrations the impact on attrition was less than that at the higher concentrations (see Table 2). This indicates that there is an optimum doping concentration to achieve a maximum overall CO<sub>2</sub> uptake. The use of XRD on the samples indicated that the concentration of the dopants was too low to be detected via this method. Therefore, the XRF technique was used to confirm the incorporation of the Cl<sup>-</sup> anion into the crystal lattice of the sorbent (see Table 2).

**4.1. Reactivity Study.** The carrying capacity of the sorbent was calculated by the ratio of the amount of CO<sub>2</sub> absorbed by the sorbent during the  $n$ th cycle and the amount of the calcined sorbent, expressed in moles or grams of CO<sub>2</sub> ( $N_{\text{CO}_2}$  or  $m_{\text{CO}_2}$ ) <sub>$n$ th</sub> per moles or grams of sorbent,  $N$ - or  $m_{\text{sorbent, calcined}}$ . Table SI 2 shows the total CO<sub>2</sub> carrying capacity over the 13 cycle tests,  $\Delta_{\text{CO}_2}$  carrying capacity and the percentage increase in total capacity over 13 and 50 cycles; these results are discussed in detail below. Of course, as the number of cycles increases to hundreds of cycles, the ratio of the total amount of CO<sub>2</sub> carried for a doped limestone to that for an undoped limestone will increasingly approximate the ratio of the residual carrying capacities.

Looking at the shape of the fit of the Grasa equation to the results of Havelock limestone, (Figure 3) interestingly  $\text{MgCl}_2$ ,  $\text{CaCl}_2$  and Grignard reagents seem to decrease in the capture capacity at first, which changes to an improved long-term reactivity afterwards. This effect has been seen before.<sup>25</sup> The total  $\text{CO}_2$  capacity of the doped samples with  $\text{MgCl}_2$ ,  $\text{CaCl}_2$  and Grignard reagent during cycle one is about 0.37, 0.39 and 0.36  $\text{g}_{\text{CO}_2}/\text{g}_{\text{CaO}}$ , respectively compared with the value of 0.42  $\text{g}_{\text{CO}_2}/\text{g}_{\text{CaO}}$  of the undoped Havelock limestone. The total  $\text{CO}_2$  capacity of the doped samples over 13 cycles was  $\sim 2.60$ ,  $2.55$  and  $2.50$   $\text{g}_{\text{CO}_2}/\text{g}_{\text{CaO}}$ , respectively while the undoped was  $\sim 2.01$   $\text{g}_{\text{CO}_2}/\text{g}_{\text{CaO}}$ , (total  $\text{CO}_2$  capacity over 13 cycles of the doped samples was  $\sim 27\%$  higher than the undoped). The fit of the Grasa equation (equation 2) for the results after 50 cycles, Figure 5, indicates that values of carrying capacity increased for the  $\text{MgCl}_2$  doped sample after the first four cycles compared to results of undoped limestone. The total  $\text{CO}_2$  capacity of the  $\text{MgCl}_2$  doped sample during the first four cycles is approximately 8% lower than the total  $\text{CO}_2$  capacity of the undoped. The total  $\text{CO}_2$  capacity of the doped sample over 50 cycles is  $\sim 6.02$   $\text{g}_{\text{CO}_2}/\text{g}_{\text{CaO}}$ , while the undoped was  $\sim 4.34$   $\text{g}_{\text{CO}_2}/\text{g}_{\text{CaO}}$  (total  $\text{CO}_2$  capacity over 50 cycles of the doped sample was  $\sim 39\%$  higher than the undoped). The curves of undoped sorbent and for doping with magnesium nitrate all show a similar shape and slope, while the  $\text{MgCl}_2$ ,  $\text{CaCl}_2$  and Grignard reagent curves even out much faster with a higher residual reactivity. The total  $\text{CO}_2$  capacity of the doped sample with  $\text{Mg}(\text{NO}_3)_2$  over 13 cycles is about 2.41  $\text{g}_{\text{CO}_2}/\text{g}_{\text{CaO}}$ , showing an increase of  $\sim 20\%$  in the total  $\text{CO}_2$  capacity over 13 cycles compared to that of the undoped).

Purbeck doped samples with  $\text{MgCl}_2$  and  $\text{CaCl}_2$  show total  $\text{CO}_2$  capacity over 13 cycles  $\sim 2.28$  and  $2.35$   $\text{g}_{\text{CO}_2}/\text{g}_{\text{CaO}}$ , respectively while the undoped was  $\sim 2.57$   $\text{g}_{\text{CO}_2}/\text{g}_{\text{CaO}}$ , (total  $\text{CO}_2$  capacity over 13 cycles of the doped samples was  $\sim 10\%$  lower than the undoped). However, the total  $\text{CO}_2$  capacity of Purbeck doped sample with 0.19 mole-%  $\text{Mg}(\text{NO}_3)_2$  dopant over 13 cycles was  $\sim 10\%$  higher than the undoped.

The mechanism of improvement could either be a chemical reaction that modifies the structure of the sorbent or an effect that changes the surface of the particle. Gonzalez *et al.* have seen similar results in their work and proposed that the dopant at first coats the reactive surface and later enhances the motility of the ions during the diffusion-controlled carbonation phase.<sup>25</sup>

As there are many possibilities for why doping enhances the cycling behaviour of a Ca-based sorbent, only some basic considerations are presented in the following. It should be noted that Table 2 demonstrates (for example) that by doping with 0.05 % MgCl<sub>2</sub> (to yield, after drying, a concentration of Cl in the doped limestone of around 0.1 %) improves the residual carrying capacity of the limestone by around 12 % (from ~3% to ~15 %). The very small dopant concentration in the limestone, post doping, indicates that the amount of CO<sub>2</sub> absorbed by the dopant directly is tiny. Changes in CO<sub>2</sub> uptake are only therefore as a result of the effects of the dopant on the limestone, not direct reaction with CO<sub>2</sub>.

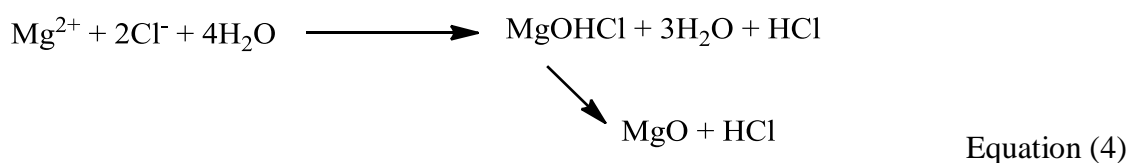
**4.2. Mechanism of Doping.** The doping process is complex and a number of factors have to be taken into account. The combination of the presence of water and heat during the doping and drying processes and the subsequent exposure to repeated calcination and carbonation cycles makes a simple determination as to where and when exactly any change of the sorbent behaviour takes place very difficult. Most probably it is not the case that a single process takes place, but a series of parallel operations.

The evaluation of the results of doping with magnesium salts suggested that if the anion and the cation both have positive effects, they appear to be additive. The more significant effect in this study is due to the Cl<sup>-</sup> anion. From these results, all examined dopants improved the long-term performance of Havelock limestone during repeated calcination/carbonation cycles, with the enhancement in the following order: MgCl<sub>2</sub> = Grignard reagent > CaCl<sub>2</sub> >> Mg(NO<sub>3</sub>)<sub>2</sub>.

Upon the doping process, using an aqueous solution,  $\text{MgCl}_2$  and  $\text{CaCl}_2$  are presented in doped limestone according to equation (3) (where M represents either  $\text{Mg}^{2+}$  or  $\text{Ca}^{2+}$ ):

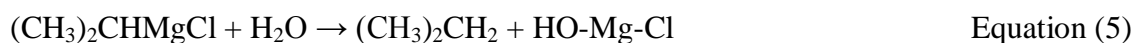


However, with the increase of temperature upon cycling the formation of  $\text{MOHCl}$  species is feasible. Previous thermal analysis studies of  $\text{MgCl}_2 \cdot 4\text{H}_2\text{O}$ <sup>26</sup> indicated the following stoichiometric equation represents the overall and predominant chemical changes occurring at the advancing reactant-product interface:

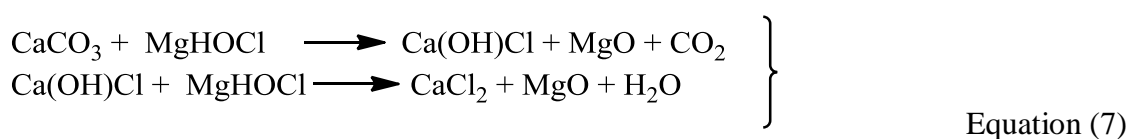


In this thermal decomposition, the intermediate formation of  $\text{MgOHCl}$  is predicted. Kinetic analysis of thermal decomposition studies<sup>26</sup> showed that the removal of  $\text{HCl}$  gas from the  $\text{MgOHCl}$  sample surface was a significant factor governing the rate of decomposition.

A similar argument holds for experiments using isopropylmagnesium chloride, a Grignard reagent. It is well documented that, in the presence of trace water and/or heat Grignard reagent decomposes, forming  $\text{MgOHCl}$ ,<sup>27</sup> equation 5 and 6, respectively.



The Cl<sup>-</sup> ion can be incorporated into the CaO crystalline matrix, enhancing the ionic diffusion and mobility of the carbonate ions through the CaCO<sub>3</sub> by straining the matrix. This is possible since the apparent ionic radius of Cl<sup>-</sup> and carbonate anion are very close, 1.81 nm for Cl<sup>-</sup> anion and 1.85 nm for carbonate anion.<sup>28</sup> It may be that MgOHCl is stabilised by, and the Cl<sup>-</sup> transferred to, the CaCO<sub>3</sub>, or alternatively that HCl diffuses into and reacts with the particles to form CaCl<sub>2</sub>, equation (7).



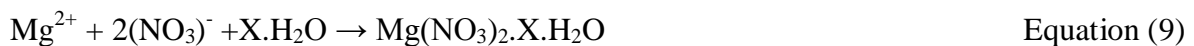
The presence of Cl<sup>-</sup> within the carbonate layer enhances sintering and changes the pore size distribution, i.e. there are physical as well as chemical effects. Ionic diffusion is a complex phenomenon associated with lattice defects (impurities or defects in the crystal structure), so any impurities or crystal defects will affect the subsequent process. As supported by the XRF analysis, the amount of Cl<sup>-</sup> ions does not increase further with increasing doping concentration above a certain optimum (see Figure SI 2). That might support the hypothesis that the sorbent cannot hold more than this amount of ions in its ionic structure and the additional amount coats the surface of the pores, potentially reducing the reactivity. The remaining unbound Cl<sup>-</sup> ions may evolve from the system upon cycling as HCl, Cl<sub>2</sub> and/or KCl, and the XRF analysis showed the decrease of K<sup>+</sup> ion upon cycling. This is in accordance with results reported previously for thermal decomposition of KCl at high temperature.<sup>29</sup> However, it is observed that the magnesium appears to have remained *in situ* to a greater extent than the chloride. This is probably owing to the production of dolomite (MgCa(CO<sub>3</sub>)<sub>2</sub>). When doping precalcined limestone, the oxygen atom of CaO is a very strongly basic anion due to its very small size and high charge which will prefer to abstract a proton from MgOHCl to generate hydroxide ions, rather than stabilising MgOHCl species. This will result in the formation of MgO and the release of Cl<sup>-</sup> ions as chlorine Cl<sub>2</sub> out of the system,

equation (8). However, there is another possibility in which CaO attacks the hydrated water molecule of the doped salt presented in the system to form Ca(OH)<sub>2</sub>. Again, neither MgOHCl nor HCl will interact with CaO and a similar decomposition mechanism will occur upon cycling.



The high mass loss observed during the reactions of calcined materials is related to high attrition due to the fragile behaviour of the calcined CaO. This observation ruled out the incorporation of the dopant into the matrix of the CaO. This is in accordance with the XRF data obtained in this work and the suggested mechanism in which there is no incorporation of the Cl<sup>-</sup> anion into the CaO matrix. In contrast, when acting on the carbonated form of the limestone, the dopant enhances sintering and therefore increases the resistance of the particles to attrition.

In order to obtain a comprehensive picture of the role of other anion species in the enhancement of the carrying capacity, the effect of the magnesium nitrate precursor on the performance of Havelock limestone was examined. Upon doping, Mg(NO<sub>3</sub>)<sub>2</sub> is presented in doped limestone according to equation (9):



Doped limestone demonstrated a minor improvement in the carrying capacity of sorbent. It is possible for ionic substitution to take place within the crystalline matrix of the CaCO<sub>3</sub>, based on the fact that, the apparent ionic radius of the NO<sub>3</sub><sup>-</sup> ion with 1.89 nm has almost the same



ionic radius of the carbonate anion with 1.85 nm.<sup>28</sup> However, the nitrate moiety is not stable upon cycling at the high temperature. This will result in the decomposition of the nitrate forming NO<sub>x</sub> species and resulted in a limited improvement in the reactivity of the sorbent by potentially forming some porosity.

**4.3. Mechanism of Reaction Extent Enhancement.** Comparison of the pore size distribution in Figure 9 for the Purbeck limestone (high initial reactivity) with that of the Havelock limestone (lower initial reactivity, more improvement), is informative. The shift of pore diameter observed during the combination of doping and cycling into a modal pore diameter of ~100 nm allows the reaction to proceed to the diffusion-limited regime, but without reducing the reactive surface area excessively, as is the case when too much dopant is added and the pore-size distribution shifts out of the area measurable by BJH analysis. This is in accordance with the work of Abanades and Alvares,<sup>30</sup> who calculated an approximate conversion limit in the fast reaction regime of around 50 nm. Of course, for Purbeck limestone, which initially contains pores of approximately twice this diameter, there is marginal improvement observed upon doping and cycling. It is also clear from the enhanced sintering observed when chloride dopes the limestone that the Cl<sup>-</sup> ion enhances the mobility of carbonate ions through the matrix.

## 5. CONCLUSION

A systematic study has been undertaken to investigate and to explore the use of different doping materials and doping methods as a reactivation strategy for limestone derived sorbents for CO<sub>2</sub> capture. A small fluidised bed reactor was constructed to subject sorbents to doping, and the doped samples were then repeatedly cycled between carbonation and calcination in a Fluidised bed reactor (FBR), and the results obtained were compared with the corresponding undoped limestone. A range of inorganic salts MgCl<sub>2</sub>, CaCl<sub>2</sub>, Mg(NO<sub>3</sub>)<sub>2</sub> and Grignard

reagent-isopropylmagnesium chloride was used in this work. Two main types of doping procedures were explored; wet impregnation, and quantitative wet impregnation. Experiments where particles of limestone were doped with small concentrations of a dopant showed a significant improvement in long-term carrying capacity; larger doping gave a marked reduction in capacity. It appears that the roles of the cation and the anion in the doping process are additive, but that the anion is more important for enhancing reactivity from the dopants investigated. A detailed mechanism to understand the doping and activation process was suggested. This relies on the shift of the pore sizes in the calcined limestone to approximately the optimal diameter for repeated reaction. For a limestone with a pore size distribution which is close to optimal, there was little improvement in reactivity upon doping. The results supported previous studies that indicated that doping could be used as an activation strategy in a fluidised environment, though care is necessary to ensure that mobile Cl<sup>-</sup> species which could enhance corrosion are not produced.

## 6. ACKNOWLEDGMENT

This work was supported by the European Community's Seventh Framework Programme (FP7/2007-2013) under GA 241302 – CaOling project.

## REERENCES

- (1) Wang, M.; Lawal, A.; Stephenson, P.; Sidders, J.; Ramshaw, C.; Post-combustion CO<sub>2</sub> capture with chemical absorption: A state-of-the-art review. *Chemical Engineering Research and Design* **2011**, *89*, 1609–1624.
- (2) Zhao, Z.; Xingyu, C.; Jinghong, M.; Ruifeng, L.; Adsorption of carbon dioxide on alkali-modified zeolite 13X adsorbents. *International Journal of Greenhouse Gas Control* **2007**, *1* (3), 355-359.
- (3) Chakravarti, S. G., A.; Hunek, B.; Advanced Technology for the Capture of Carbon Dioxide from Flue Gases. In *First National Conference on Carbon Sequestration*, Washington, DC, 2001.
- (4) Blamey, J. A., E.J.; Wang, J.; Fennell, P. S., The calcium looping cycle for large-scale CO<sub>2</sub> capture. *Progress in Energy and Combustion Science* **2010**, *36* (2), 260-279.
- (5) Dean, C. C. B., J.; Florin, N. H.; Al-Jeboori, M. J.; Fennell, P. S.; The calcium looping cycle for CO<sub>2</sub> capture from power generation, cement manufacture and hydrogen production. *Chemical Engineering Research and Design* **2011**, *89*, 836-855.
- (6) Development of postcombustion CO<sub>2</sub> capture with CaO in a large testing facility, EU FP7 funded project, La Pereda, Spain, (Opening day 19 April 2012). (7) Borgwardt, R. H.; Sintering of nascent calcium oxide. *Chemical Engineering Science* **1989**, *44* (1), 53-60.
- (8) González, B.; Alonso, M.; Abanades, J. C.; Sorbent attrition in a carbonation/calcination pilot plant for capturing CO<sub>2</sub> from flue gases. *Fuel* **2010**, *89* (10), 2918-2924.
- (9) Manovic, V.; Anthony, E. J.; Thermal Activation of CaO-Based Sorbent and Self-Reactivation during CO<sub>2</sub> Capture Looping Cycles. *Environ. Sci. Technol.* **2008**, *42* (11), 4170-4174.
- (10) Manovic, V.; Anthony, E. J.; Loncarevic, D.; CO<sub>2</sub> looping cycles with CaO-based sorbent pretreated in CO<sub>2</sub> at high temperature. *Chemical Engineering Science* **2009**, *64* (14), 3236-3245.
- (11) Dobner, S.; Sterns, L.; Graff, R. A.; Squires, A. M.; cyclic Calcination and Recarbonation of Calcined Dolomite. *Industrial & Engineering Chemistry Process Design and Development* **1977**, *16* (4), 479-486.
- (12) Sun, P.; Grace, J. R.; Jim, L. C.; Anthony, E. D.; Investigation of attempts to improve cyclic CO<sub>2</sub> capture by sorbent hydration and modification. *Industrial & Engineering Chemistry Research* **2008**, *47* (6), 2024-2032.
- (13) Li, Y.-j.; Zhao, C.-s.; Duan, L.-b.; Liang, C.; Li, Q.-z.; Wu, Z.; Chen, H.-c.; Cyclic calcination/carbonation looping of dolomite modified with acetic acid for CO<sub>2</sub> capture. *Fuel Processing Technology* **2008**, *89* (12), 1461-1469.
- (14) Dennis, J. S.; Pacciani, R.; The rate and extent of uptake of CO<sub>2</sub> by a synthetic, CaO-containing sorbent. *Chemical Engineering Science* **2009**, *64* (9), 2147-2157.
- (15) Fennell, P. S.; Pacciani, R.; Dennis, J. S.; Davidson, J. F.; Hayhurst A. N.; The effects of repeated cycles of calcination and carbonation on a variety of different limestones, as measured in a hot fluidized bed of sand. *Energy & Fuels* **2007**, *21* (4), 2072-2081.
- (16) Salvador, C. L. D.; Anthony, E.J.; Abanades, J. C.; Enhancement of CaO for CO<sub>2</sub> capture in an FBC environment. *Chemical Engineering Journal* **2003**, *96* (1-3), 187-195.
- (17) Reddy, E. P.; Smirniotis, P. G.; High-temperature sorbents for CO<sub>2</sub> made of alkali metals doped on CaO supports. *Journal of Physical Chemistry B* **2004**, *108* (23), 7794-7800.
- (18) Li, Y.; Zhao, C.; Chen, H.; Duan, L.; Chen, X.; Cyclic CO<sub>2</sub> capture behavior of KMnO<sub>4</sub>-doped CaO-based sorbent. *Fuel* **2010**, *89* (3), 642-649.

- (19) Elzinga, G. D.; Reijers, H. T. J.; Cobden, P. D.; Haije, W. G.; Van Den Brink, R. W.; CaO sorbent stabilisation for CO<sub>2</sub> capture applications. In *Energy Procedia*, 2011; Vol. 4, pp 844–851.
- (20) Megaritis, A.; Zhuo, Y.; Messenböck, R.; Dugwell, D. R.; Kandiyoti, R.; Pyrolysis and gasification in a bench-scale high-pressure fluidized-bed reactor *Energy & Fuels* **1998**, *12* (1), 144-151.
- (21) Grasa, G. S.; Abanades, J. C.; CO<sub>2</sub> capture capacity of CaO in long series of carbonation/calcination cycles. *Industrial & Engineering Chemistry Research* **2006**, *45* (26), 8846-8851.
- (22) Wen, C.Y.; Yu, Y. H.; A generalized method for predicting the minimum fluidization velocity. *AIChE J* **1966**, *12* (3), 610-612.
- (23) Brunauer, S.; Emmett, P. H.; Teller, E.; Adsorption of Gases in Multimolecular Layers. *Journal of the American Chemical Society* **1938**, *60* (2), 309-319.
- (24) Barrett, E. P.; Joyner, L. G.; Halenda, P. P.; The Determination of Pore Volume and Area Distributions in Porous Substances. I. Computations from Nitrogen Isotherms. *Journal of the American Chemical Society* **1951**, *73* (1), 373-380.
- (25) Gonzalez, B.; Blamey, J.; McBride-Wright, M.; Carter, N.; Dugwell, D.; Fennell, P.; Abanades, J. C.; Calcium looping for CO<sub>2</sub> capture: sorbent enhancement through doping. *Energy Procedia* **2011**, *4*, 402-409.
- (26) Kashani-Nejad, S. N., K.-W.; Harris, R.; MgOHCl Thermal Decomposition Kinetics. *Metallurgical & Materials Transactions B* **2005**, *36B*, 153-157.
- (27) Carson, A. S.; Skinner, H. A.; Heat of Formation of the Grignard Reagent, CH<sub>3</sub>MgI: Ether. *Nature* **1954**, *165*, 484.
- (28) Manku, G. S.; *Theoretical Principles of Inorganic Chemistry*. 22<sup>nd</sup> Edition ed.; Pulished by Tata McGraw-Hill Publishing Company limited, : New Delhi, 2006.
- (29) Castro, M. A.; Faulds, K.; Smith, W. E.; Aller, A. J.; Littlejohn, D.; Characterization of condensed phase species produced during the thermal treatment of metal chlorides on a graphite platform using surface analysis techniques. *Spectrochimica Acta Part B: Atomic Spectroscopy* **2004**, *59* (12), 1935-1942.
- (30) Abanades, J. C.; Alvares, D; Conversion limits in the Reaction of CO<sub>2</sub> with Lime. *Energy & Fuels* **2003**, *17*, 308 - 315.

## Figure Captions

**Figure 1.** Schematic diagram of the experimental apparatus.

**Figure 2.** Carrying capacity (normalised) for Havelock limestone, plotted against the number of cycles (the lines represent the fitting via equation 2); ( $\square$ ) undoped, ( $\ominus$ ) 0.05M  $\text{MgCl}_2$  wet impregnation, ( $\times$ ) 0.165 mol-%  $\text{MgCl}_2$  quantitative wet impregnation .

**Figure 3.** Carrying capacity (normalised) for Havelock limestone, plotted against the number of cycles (the lines represent the fitting via equation 2); ( $\square$ ) undoped, ( $\diamond$ ) 0.159 mol-%  $\text{Mg}(\text{NO}_3)_2$ , ( $\times$ ) 0.165 mol-%  $\text{MgCl}_2$ , ( $\triangleright$ ) 0.138 mol-%  $\text{CaCl}_2$ , ( $\circ$ ) 0.15 mol-% Grignard reagent.

**Figure 4.** Carrying capacity (normalised) for Havelock limestone, plotted against the number of cycles; ( $\square$ ) undoped, ( $\diamond$ ) 0.755 mol-%  $\text{MgCl}_2$ , ( $\times$ ) 0.224 mol-%  $\text{MgCl}_2$ , ( $\triangle$ ) 0.165 mol-%  $\text{MgCl}_2$ , ( $\circ$ ) 0.12 mol-%  $\text{MgCl}_2$ . Error bars represent standard deviation between repeated experiments.

**Figure 5.** Carrying capacity (normalised) for Havelock limestone, plotted against 50 cycles; ( $\bullet$ ) undoped, ( $\triangle$ ) 0.165 mol-%  $\text{MgCl}_2$ .

**Figure 6.** Carrying capacity (normalised) for Purbeck limestone, plotted against the number of cycles (the line represent the fitting via equation 2); ( $\times$ ) undoped, ( $\triangleleft$ ) 0.165 mol-%  $\text{MgCl}_2$ , ( $\circ$ ) 0.138 mol-%  $\text{CaCl}_2$ , ( $\bullet$ ) 0.19 mol-%  $\text{Mg}(\text{NO}_3)_2$ .

**Figure 7.** Carrying capacity (normalised) for Havelock limestone, plotted against the number of cycles (the line represent the fitting via equation 2); ( $\triangleright$ ) undoped, ( $\times$ ) 0.165mol-%  $\text{MgCl}_2$ , -  $\text{CaCO}_3$ , ( $\triangleleft$ ) 0.15 mol-% Grignard reagent -  $\text{CaCO}_3$ , ( $\square$ ) 0.138 mol-%  $\text{CaCl}_2$  -  $\text{CaCO}_3$ , ( $\bullet$ )

0.15 mol-% Grignard reagent – CaO, ( $\Delta$ ) 0.165 mol-%  $\text{MgCl}_2$ , -CaO. ( $\diamond$ ) 0.138 mol-%  $\text{CaCl}_2$  – CaO.

**Figure 8.** Carrying capacity (normalised) for Purbeck limestone, plotted against the number of cycles (the line represent the fitting via equation 2); ( $\triangleleft$ ) undoped, ( $\square$ ) doped with 0.101 mol-%  $\text{Mg}(\text{NO}_3)_2$ , (O) doped with 0.143 mol-%  $\text{Mg}(\text{NO}_3)_2$ , (X) doped with 0.165 mol-%  $\text{Mg}(\text{NO}_3)_2$ , ( $\Delta$ ) doped with 0.19 mol-%  $\text{Mg}(\text{NO}_3)_2$ , (+) doped with 0.2.06 mol-%  $\text{Mg}(\text{NO}_3)_2$ .

**Figure 9.** Differential pore size distribution (V ) volume of pores : (A) Havelock, (—) undoped, (— $\Delta$ —) doped with 0.165 and (— $\bullet$ —) doped with 0.76 mole-%  $\text{MgCl}_2$ ; (b) Purbeck, (—) undoped, (-----) doped with 0.10, (—) doped with 0.16 and (— $\square$ —) doped with 0.19 mole-%  $\text{Mg}(\text{NO}_3)_2$ .

**Figure 10.** BET surface areas measured for the doped limestones in their calcined states, plotted against the concentration of doping solution in mole-%: ( $\blacktriangle$ ) Purbeck doped with  $\text{Mg}(\text{NO}_3)_2$ , ( $\bullet$ ) Havelock doped with  $\text{MgCl}_2$ .

**Figure 11.** (A) Scanning electron microscope image of the doped of particles of Havelock limestone with 0.5 M  $\text{MgCl}_2$  solution: (B) Doped element percentage at approximate distance (700  $\mu\text{m}$ ) from P1(2) across particles P1(12), (\*) atomic % Mg and ( $\blacklozenge$ ) atomic % Cl.

**Figure 12.** Mass loss in percentage against concentration of doping solution in mole-% after 13 cycles; ( $\bullet$ ) Purbeck doped with  $\text{Mg}(\text{NO}_3)_2$ ; ( $\blacksquare$ ) Havelock doped with  $\text{MgCl}_2$ ; ( $\blacktriangle$ ) Havelock doped with  $\text{Mg}(\text{NO}_3)_2$ .

## Table Captions

**Table 1.** Chemical Composition of Limestones in wt-%.

**Table 2.** Summary of experimental measurements and conditions; QWI = Quantitative Wet Impregnation, WI = Wet Impregnation, SM = Solid Mixing, C. C. = Carrying Capacity, SD = Standard Deviation, \* = Cl<sup>-</sup> ion % of the uncycled doped sample measured using XRF after dried in an oven at 273 k.

**Table 3.** XRF data in mole-% for Havelock: undoped/uncycled, undoped/13 cycles, doped with 0.15 mole-% Grignard reagent/13 cycles, doped with 0.138 mole-% CaCl<sub>2</sub>/13 cycles, doped with 0.165 mole-% MgCl<sub>2</sub>/13 cycles.

**Table 4.** XRF data in mole-% for Purbeck: undoped/uncycled, undoped/13 cycles, doped with different mole-% Mg(NO<sub>3</sub>)<sub>2</sub>/13 cycles.

## Figures

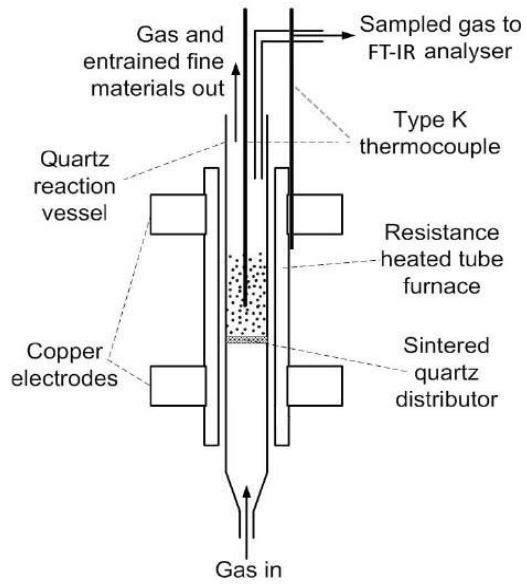


Figure 1

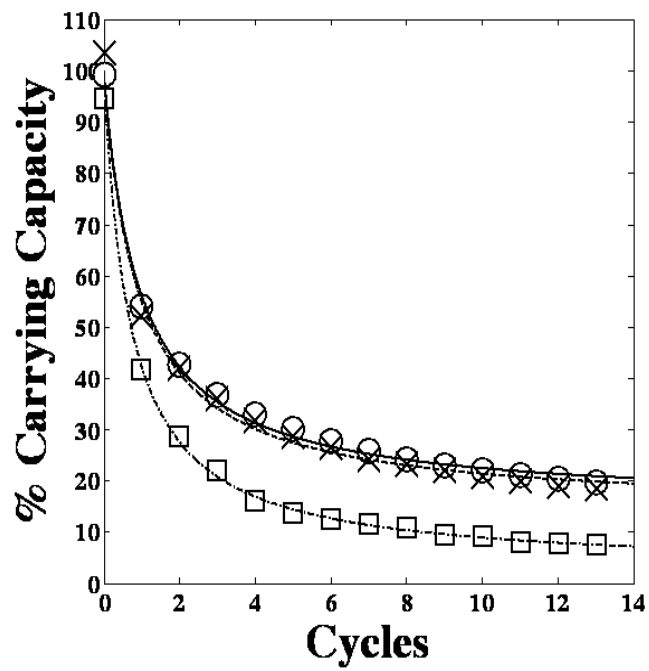


Figure 2



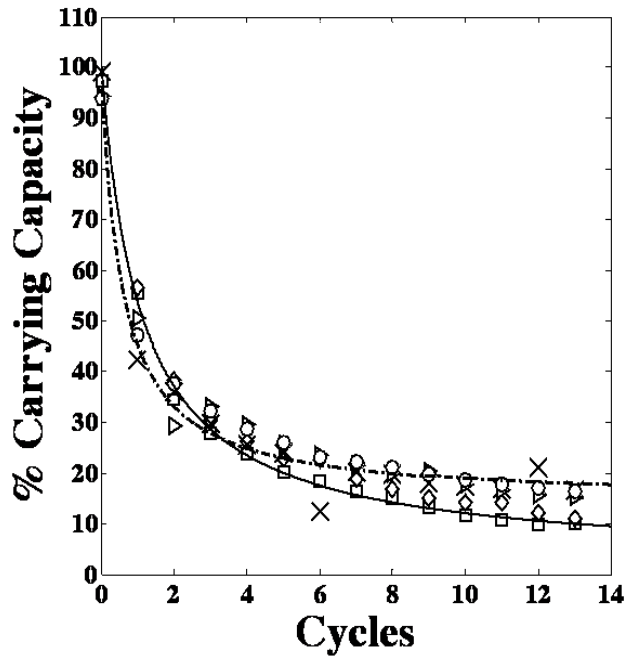


Figure 3

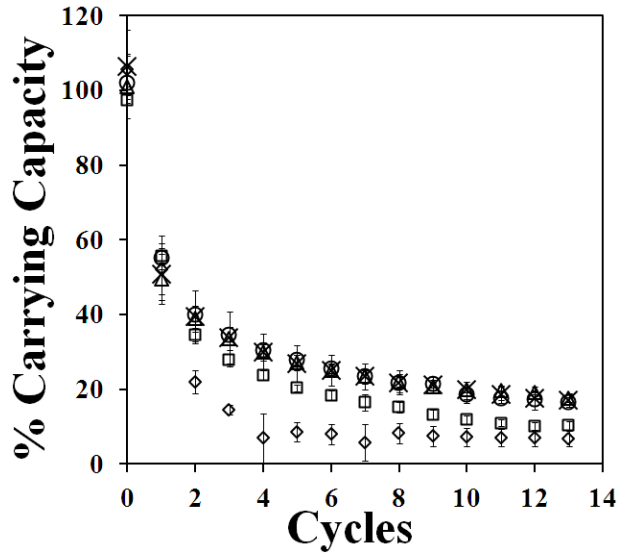


Figure 4

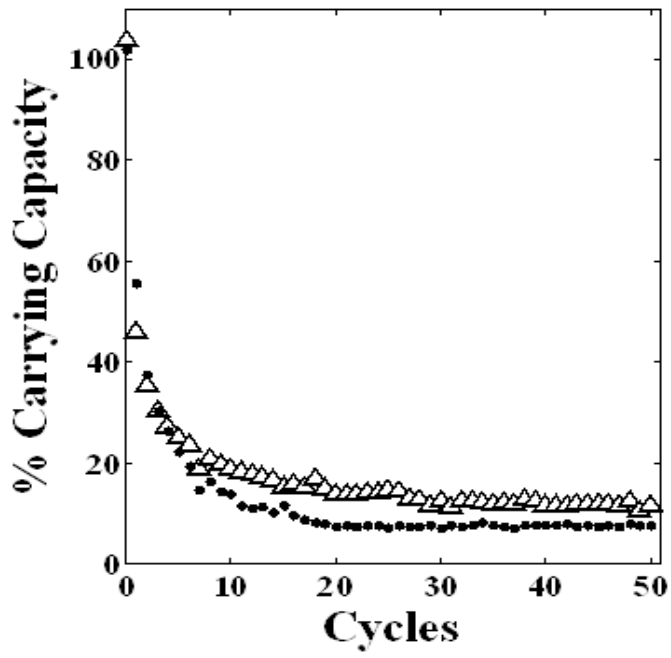


Figure 5

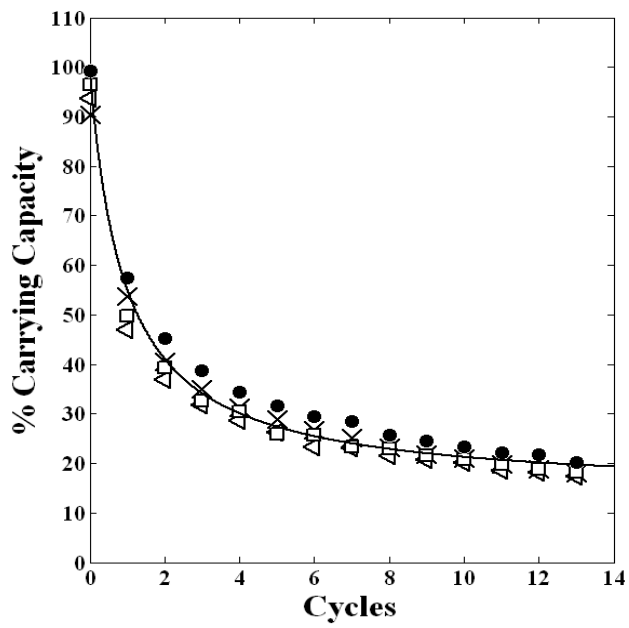


Figure 6

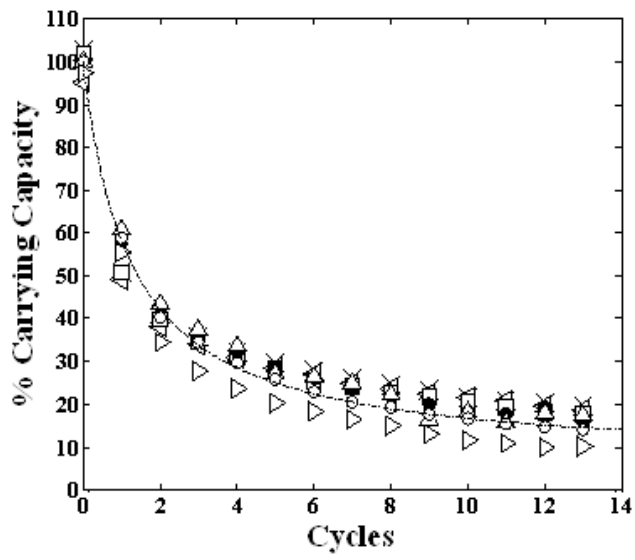


Figure 7

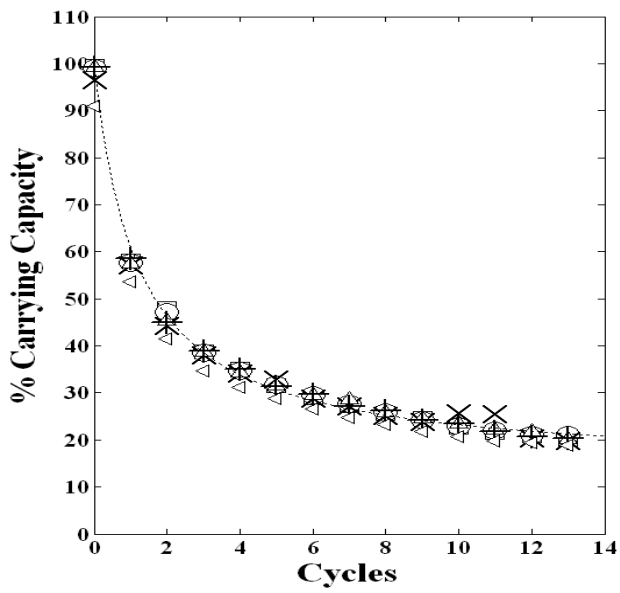
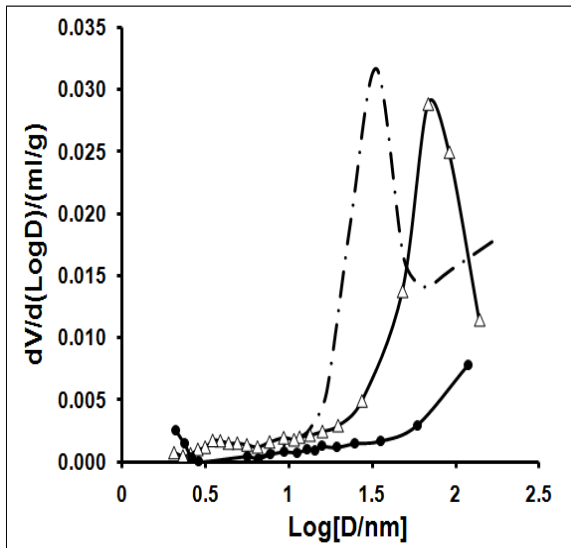
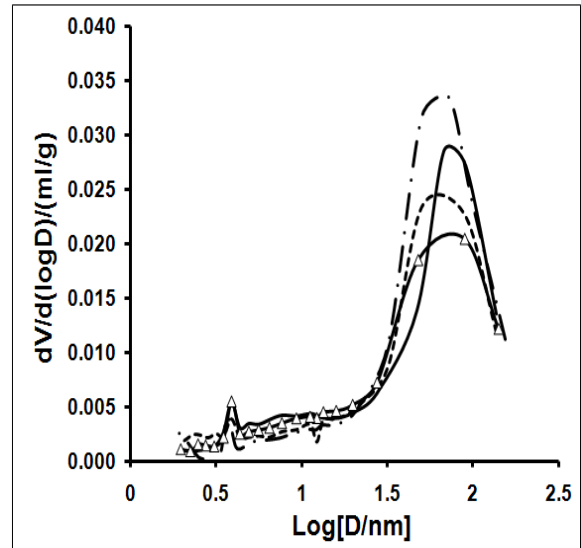


Figure 8



A



B

Figure 9

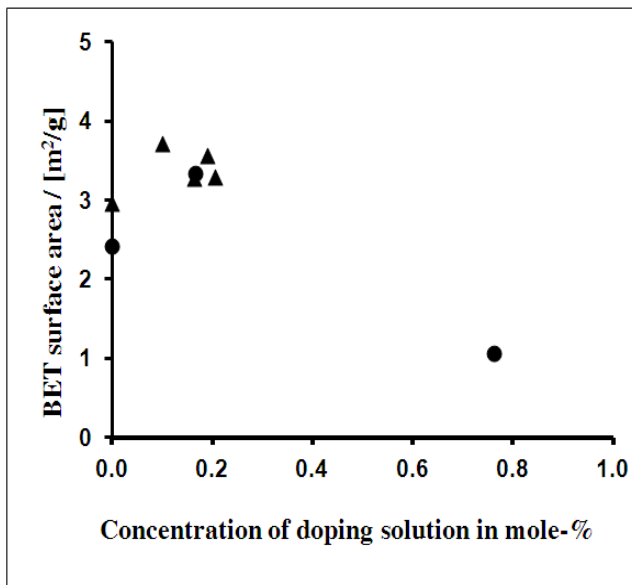
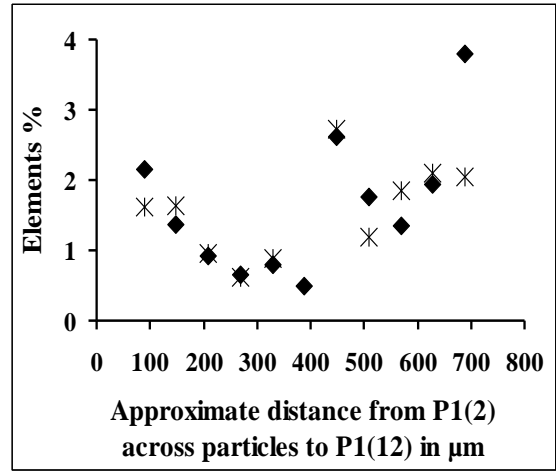
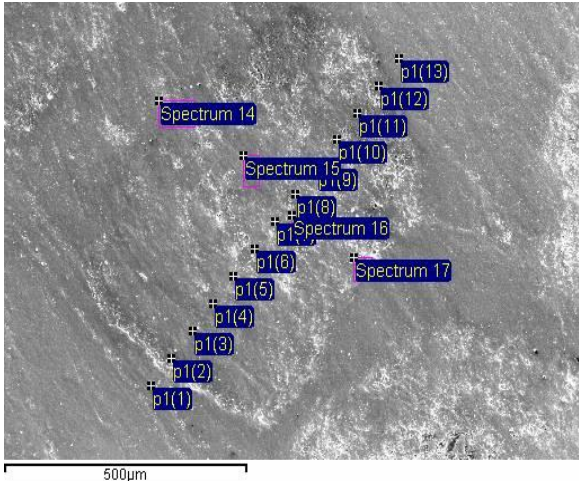


Figure 10



A

B

Figure 11

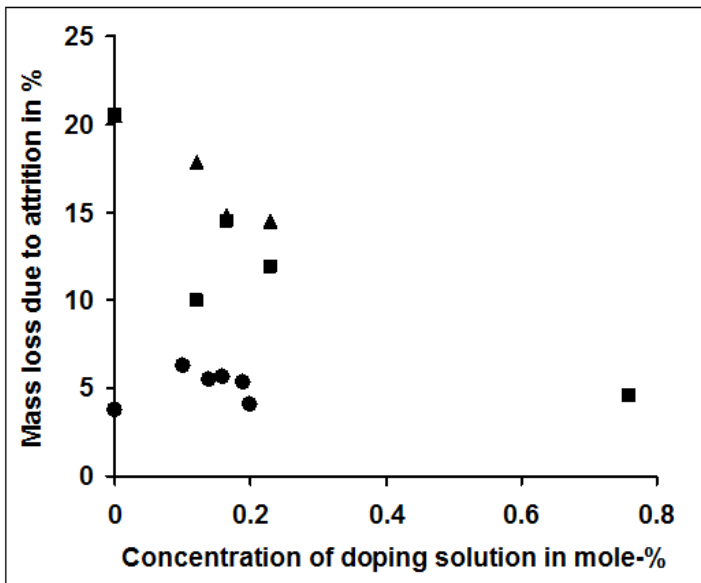


Figure 12

## Tables

**Table 1**

<b>Component</b>	<b>Havelock</b>	<b>Purbeck</b>
CaCO <sub>3</sub>	97.63	92.32
SrO	0.03	0.04
SiO <sub>2</sub>	1.45	6.23
MnO	0.16	0.03
MgO	0.23	0.54
K <sub>2</sub> O	0.05	0.08
Fe <sub>2</sub> O <sub>3</sub>	0.16	0.28
Al <sub>2</sub> O <sub>3</sub>	0.29	0.36
S	0.00	0.05
P	0.00	0.07

**Table 2**

<b>Limestone</b>	<b>Dopant</b>	<b>Concentration of dopant mole-%</b>	<b>C.C. after 13 or 50 cycles (1 SD)</b>		<b>Asymptotic C. C. % (Grasa)</b>	<b>Mass loss <math>\Delta m</math> %</b>	<b>Total added Cl<sup>-</sup> ion % (XRF)*</b>	<b>Cl<sup>-</sup> ion % after 13 cycles (XRF)</b>	
<b>Havelock (carbonated)</b>	Undoped	0	10.22	(0.22)	2.5	20.08	-	-	
	MgCl <sub>2</sub> QWI	0.165	17.63	(1.28)	14.38	14.51	0.33	0.06	
		0.755	6.76	-2.3	4.62	1.51	0.10		
	50 Cycles	0.00	7.58		4.30	20.08	-	-	
	50 Cycles QWI	0.0165	11.72		10.82	13.56	-	-	
		WI	0.02	16.29	(0.18)	10.05	9.51	0.10*	0.00
			0.05	20.64	(0.90)	15.13	5.30	0.10*	0.06
	0.50		7.59		2.74	3.70	0.90*	0.24	
	Grignard Reagent	QWI	0.15	17.31	(0.21)	13.29	14.41	0.15*	0.06
	CaCl <sub>2</sub> QWI	0.138	16.53	(0.61)	13.16	7.28	0.27	0.07	
		0.361	12.09		10.76	10.77	0.72	0.06	
	Mg(NO <sub>3</sub> ) <sub>2</sub> QWI	0.159	12.37	(0.28)	5.20	15.39	-	-	
		0.216	9.33		2.4	15.39	-	-	

**Table 2. Continued.**

<b>Limestone</b>	<b>Dopant</b>		<b>Concentration of dopant mole-%</b>	<b>C. C. after 13 or 50 cycles (1 SD)</b>		<b>Asymptotic C. C. % (Grasa)</b>	<b>Mass loss <math>\Delta m</math> %</b>	<b>Total added Cl<sup>-</sup> ion % (XRF)*</b>	<b>Cl<sup>-</sup> ion % after 13 cycles (XRF)</b>
<b>Havelock (calcined)</b>	MgCl <sub>2</sub>	SM	0.165	16.25		7.73	23.92	0.33	0.0
	CaCl <sub>2</sub>	SM	0.138	14.20		6.40	30.11	0.27	0.0
	Grignard Reagent	QWI	0.15	15.73		10.05	32.87	0.15*	0.0
<b>Purbeck</b>	Undoped		0	19.86		13.79	3.66	-	-
	Mg(NO <sub>3</sub> ) <sub>2</sub>	QWI	0.143	21.08		15.28	5.35	-	-
			0.19	20.83	(0.92)	16.08	5.21	-	-
	MgCl <sub>2</sub>	QWI	0.165	17.38	(1.57)	14.75	3.52	0.33	0.0
			0.755	14.43		14.12	4.22	1.51	0.07
CaCl <sub>2</sub>	QWI	0.138	17.82	(0.65)	15.01	1.77	0.27	0.0	
		0.165	16.12		15.32	2.88	0.34	0.07	



**Table 3**

<b>Composition</b>	<b>CaCO<sub>3</sub>, uncycled</b>	<b>CaO, 13 cycles</b>	<b>CaCO<sub>3</sub>+ Grignard, 13 cycles</b>	<b>CaCO<sub>3</sub> + CaCl<sub>2</sub>, 13 cycles</b>	<b>CaCO<sub>3</sub>+ MgCl<sub>2</sub>, 13 cycles</b>
CaCO <sub>3</sub> /CaO	96.38	97.41	96.43	96.40	96.71
SrO <sub>2</sub>	0.03	0.03	0.03	0.03	0.03
SiO <sub>2</sub>	2.38	1.71	2.30	2.30	2.06
MnO <sub>2</sub>	0.22	0.22	0.28	0.33	0.29
MgO	0.55	0.47	0.59	0.53	0.51
K <sub>2</sub> O	0.06	0.05	0.02	0.02	0.02
Fe <sub>2</sub> O <sub>3</sub>	0.10	0.10	0.10	0.12	0.11
Al <sub>2</sub> O <sub>3</sub>	0.28	0.02	0.20	0.21	0.21
HCl	0	0	0.06	0.07	0.06

**Table 4**

<b>Composition</b>	<b>CaCO<sub>3</sub> uncycled</b>	<b>CaO Undoped/ cycled</b>	<b>Mg(NO<sub>3</sub>)<sub>2</sub></b>	<b>Mg(NO<sub>3</sub>)<sub>2</sub></b>	<b>Mg(NO<sub>3</sub>)<sub>2</sub></b>	<b>Mg(NO<sub>3</sub>)<sub>2</sub></b>	<b>Mg(NO<sub>3</sub>)<sub>2</sub></b>
Dopant mole - %	0.000	0.00	0.101	0.143	0.165	0.190	0.206
CaO	92.80	88.13	89.90	90.23	90.36	90.32	89.00
SrO <sub>2</sub>	0.02	0.03	0.03	0.03	0.03	0.03	0.03
SiO <sub>2</sub>	5.85	9.83	7.88	7.51	7.38	7.33	8.68
MnO <sub>2</sub>	0.03	0.04	0.04	0.04	0.04	0.04	0.04
MgO	0.76	1.27	1.39	1.50	1.51	1.58	1.56
K <sub>2</sub> O	0.05	0.03	0.03	0.03	0.03	0.03	0.03
Fe <sub>2</sub> O <sub>3</sub>	0.10	0.17	0.17	0.17	0.17	0.17	0.19
Al <sub>2</sub> O <sub>3</sub>	0.20	0.27	0.33	0.26	0.25	0.26	0.26
S	0.08	0.07	0.07	0.07	0.06	0.07	0.06
P	0.12	0.16	0.17	0.17	0.17	0.16	0.16